RSC Advances

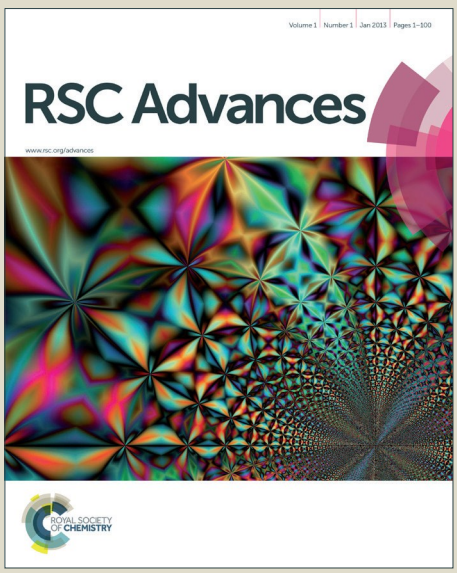

ROYAL SOCIETY OF CHEMISTRY

www.rsc.org/advances

Performance of hybrid nanostructured conductive cotton threads as LPG sensor at ambient temperature: Preparation and analysis

N.G. Shimpi*[2], D.P. Hansora[1], R. Yadav[1], S. Mishra[1]

[1]*University Institute of Chemical Technology, North Maharashtra University, Jalgaon-425001*

[2]*Department of Chemistry, University of Mumbai, Kalina, Santacruz East, Mumbai-400098 Maharashtra, India*

***Corresponding Author:**

Dr. Navinchandra Shimpi, Phone No: +91-22-26543575

Email ID: navin_shimpi@rediffmail.com

ABSTRACT

The present research work explores the feasibility of novel sensor based on nanostructured cotton threads. These threads were functionalized using carbon nanotubes (CNTs) and PAni/γ-Fe_2O_3 nanostructures. At to begin with, we prepared catalyst nanoparticles by hydrothermal method. These nanofabricated catalyst particles were used to grow CNTs by newly designed catalytic chemical vapor deposition set up. The resulting CNTs were subjected to strategical purification steps. Both nanofabricated catalyst and decontaminated CNTs were analysed to study their size, shape, surface morphology and crystalline structure. Pure CNTs were successfully incorporated on permeable cotton threads using basic submersion in a CNT-ink under ultrasound environment. These profoundly conductive cotton threads were functionalized using PAni/γ-Fe_2O_3 nanostructures by facile ultrasound assisted *in-situ* polymerization. The hybrid nanostructured cotton threads were prepared at different loadings of both CNTs and PAni/γ-Fe_2O_3 nanocomposites and their influence was further investigated to study their surface morphology, electrical behavior and sensing performance for detection of LPG. Quick response time and maximum response value (R_{res} = 0.91) were observed for low concentration (50 ppm) detection of LPG at ambient temperature. So these hybrid nanostructured cotton based sensing threads could be easily woven into the textile materials which will be useful as wearable gadgets for LPG detection in households' kitchens, its manufacturing sites and industries. Also this work will boost an essential encouragement for the development of wearable smart sensing gadgets.

Keywords: CNT, polymer nanocomposites, Hybrid thread, wearable sensor

1 Introduction

Leakages of explosive gases have become a great cause of concern for environmental pollution. As the liquefied petroleum gas (LPG) is a mix composition of hydrocarbons (propane and butane) and highly inflammable gas, its air pollution affects the health through irritated respiratory tract, nose and eyes. LPG is regularly used as a cooking fuel in household purposes, vehicles, agriculture and industrial production sites and thus accidental explosion due to its leakages has sharply increased. These could be very dangerous for the property and threat to human lives. So to overcome these significant hassle, it is imperative to develop fast and selective detection with precise monitoring that could avoid any LPG leakage at low concentrations (ppm) and thus be beneficial in preventing the occurrence of accidental explosions, any fire hazards and losses. The National Institute for Occupational Safety and Health (NIOSH) and Occupational Safety and Health Administration (OSHA) have specified lower explosive limit (LEL) standards for chemical hazards that is 21,000 ppm (2.1 % by volume in air) for propane and 19,000 ppm (1.9 % by volume in air) for butane. The NIOSH and OSHA have also set permissible exposure limit (PEL) standards for LPG as 1000 ppm (0.1 % by volume in air). Limit below this level can be detected if a safety device like high sensitive and quick time LPG sensor is put in place. Reliable sensors with improved gas response have been developed to monitor and precisely measure leakages. But, at certain low permissible concentration of LPG, some metal oxides/sulfides and ceramic based LPG sensors have shown poor performance with respect to the sensitivity, response and recovery times, long term stability, selectivity, high power consumption, complex fabrication and high cost for the detection and generally operate above room temperature. Consequently, there is a need for development of cost effective sensors to monitor LPG of the lowest possible concentration at room temperature (~30 ^{o}C). The detection of LPG at room temperature will be definitely helpful for the households, safety for vehicles, chemical industries and research

laboratories. To overcome these draw backs, conducting polymers (CPs) and nanostructures (such as nanoparticles, nanotubes, nanosheets, nanoflowers and nanowalls) have been recently investigated as effective materials for room temperature chemical sensors which have favorable properties such as easy processability, degree of miniaturization [1-20].

Sensing technology [21-26] has become more significant because of various sensing methods (based on different materials and techniques) and their widespread smart wearable applications. Xiao et al [22] summarized the comparison of various sensing materials and methods, along with their performance, advantages and disadvantages [22]. Various forms of nanocarbon have been demonstrated their potential for sensing applications owing to their better electrical conductivity [27-28]. The carbon nanotubes (CNTs) possess extraordinary and excellent characteristics [29-30] such as electrical, mechanical, thermal, electronics, vibrational, optical and electromechanical properties which corroborate their potential in variety of applications [29,31-32] in flat panel displays, energy storage, field emission devices, electrochemical, electronic gadgets and sensors [30,33-40]. CNT is an intriguing nano-cylindrical form of rolled carbonaceous graphene sheet and capped their both ends by half fullerene molecule. It has also shown its potential as a sensing element in various nano-electro mechanical sensors such as chemical sensors, temperature sensors, mass sensors, pressure sensors, flow sensors and biosensors. These CNT based sensors have been investigated, which indicate that properties of CNTs can play a vital role when designing the sensors [29,34-52]. Hybrid nanocomposites based on chitosan grafted by CNT and graphene oxide have demonstrated their potential for vapor sensing of organic compounds [53] and drug delivery [54], while CNT ink can detect of hydrogen peroxide and NADH (β-nicotinamide adenine dinucleotide) [41]. The doped CNTs have been also utilized for the applications of nanosensors to detect CO_2, CH_4, CO and water molecules with good response at room temperature [42-43,55]. MWCNTs grown on iron catalyst nanoparticles can be used for sensing applications [56-57].

Because of extreme sensitive perturbations and electric properties of SWCNTs, their nanoscopically functionalized hybrid layers (with the transition metals Au, Ag, Co, Fe, Mn, Ni, Pd, Pt and Ti) based sensors were used to detect vapor of alcohol, NH_3, NO_2, CO and C_6H_6 at room temperature [44-51]. In the recent years, many efforts have been put forth for metal oxide and sulfide based gas sensors such as Fe_2O_3 [1], Bi_2O_3 and Y_2O_3 [2], SnO_2 [2,9], TiO_2 [4-5,13], ZnO [7-8,14], $ZnMoO_4$[10], CdSe [12], $ZnFe_2O_4$ [17], CdS [3,16,18,58], PbS [18]. Semiconducting materials like Fe_2O_3 nanostructures [1] and nanostructured SnO_2 hollow spheres [2] have been used for LPG sensing at room temperature. Similarly, CP such as polypyrrole (PPy) [58], nanostructures and fibres of PAni [1,3-4,6-7,10-12,14-15,26,59] are promising polymeric material for sensing applications. PAni–CNT composites are reported as pH sensor for the detection of triethylamine, nitrite vapour, CO_2, acetaminophen present in acetate, glucose, ascorbic acid, H_2O_2, NH_3, H_2S, acetic acid, hydrazine. These sensors are useful for detection in industrial monitoring, personal safety, and medical field [37,52,60].

Nanocarbon-based gas sensors bear tremendous flexibility that makes them ideal and suitable candidates, e.g. super-stretchable spring-like CNT ropes for the next generation gas/chemical sensors [61-62]. Porous cotton threads are made profoundly conductive using basic submersion of a CNT without affecting its shape because CNTs have solid Van der Waals interactions with this sort of poly-D glucose chains based micro fibrils. The permeable conductive textiles have been receiving immense interest for smart wearable devices. These wearable applications include (i) energy storage device [63], (ii) electronics and yarn based ammonia sensor [23], (iii) multi-grade nanostructured (PPy-MnO_2-CNT) cotton thread base wearable supercapacitor [64], (iv) wearable electrochemical devices for detection of K^+ and NH_4^+, pH [24], (v) cable-type polyelectrolyte-wrapped graphene/CNT core-sheath fibre based supercapacitor [65], (vi) metal-free fiber-based generator (FBG) based smart garments [66], (vii) highly sensitive, stretchable and wearable multifunctional sensors (based on conductive electrodes of silver

nanowires and dielectric made from Ecoflex) for healthcare and flexible touch panel [67], (viii) triboelectric generator (TEG) for an energy harvesting device interconnected by conductive threads as wearable electronics [68], (ix) stretchable electronic devices made from CNTs for detection of human motion, including typing, body movement, speech and breathing [69], (x) CNT based elastic strain sensors and robust rotational actuators [70], (xi) cotton fiber/textile structures as wearable electronic devices with mechanical functionalities [71], (xii) smart fabric sensor as electronic textiles [25] and (xiii) wearable textile-based battery rechargeable by solar energy [72]. *In-situ* polymerized PPy/cotton fabric based conducting textiles possess high conductivity, and shallow skin depth [58,73]. The flexible sensors were fabricated on 100-μm thick polyimide foils which can withstand mechanical deformations. This beneficiary concept can be useful for instance safety applications for objects located in a dangerous environment to avoid direct access by hand [74].

1.1 Aims of these research work.

We have reviewed various fabrication techniques, properties and application of hybrid nanostructured conductive cotton threads and reported in detail in part I of this paper. From the above aforementioned previous research perspectives and motivation (discussed in section S1 of supplementary information) from past work, we have demonstrated strategical methods for the development of hybrid nanostructured conductive cotton threads which were investigated for LPG sensing at room temperature. This research work includes preparation of Fe/MgO catalyst nanoparticles by hydrothermal method, preparation of CNTs by newly designed chemical vapor deposition (CVD) set up followed by their successive purification. Characterization and analysis of catalyst nanoparticles and CNTs are also discussed which determine size and shape, growth mechanism and crystalline structure. Pure CNTs were variably incorporated on surface of a flexible cotton thread by ultrasound sonication route.

Ultrasound assisted *in-situ* chemical polymerization route was preferred for the preparation of PAni/γ-Fe_2O_3 nanostructures. These polymer nanostructured composites were embedded in variable amount on conductive threads by ultrasound assisted dipping and coating method. Pure CNTs, PAni/γ-Fe_2O_3 nanostructures and CNT/PAni/γ-Fe_2O_3 nanostructured threads were studied for thermal stability and electrical current-voltage (I-V) characteristics. Meanwhile, gas sensing performances like response value, response time and recovery time, selectivity of composition, sensing mechanism were studied to assess the feasibility of hybrid nanostructured cotton threads for detection of LPG at room temperature.

1.2 Importance of the current research work

The research gives idea about hybrid nanostructured cotton threads and its feasibility towards detection of 50 ppm LPG at room temperature. This research work is important, because CNT and PAni/γ-Fe_2O_3 nanostructures were embedded on cotton threads first time by ultrasound assisted dipping and coating method and *in-situ* polymerization under ultrasound environment. Fast recovery and quick response time have been achieved by functionalizing cotton threads using hybrid (CNT/PAni/γ-Fe_2O_3) nanostructures owing to their nanoscale morphology and expansive surface. These achieved results are also significant because as wt% loading of CNT increases the conductivity of hybrid nanostructured thread improves, which is the crucial parameter for higher response value towards low concentration (50 ppm) of LPG detection at ambient temperature. Higher loading of (CNT/PAni/γ-Fe_2O_3) nanostructures on the surface of cotton threads showed maximum response value (0.91) towards low concentration (50 ppm) of LPG. These hybrid nanostructured threads could be an efficient sensor for detection of LPG at room temperature. Meanwhile, it can be woven in to textile garments and also be useful as wearable gadgets for LPG detection in households' kitchens and manufacturing sites.

2 Experimental

2.1 Materials and reagents.

Iron (III) nitrate [$Fe(NO_3)_3 \cdot 9H_2O$] (Rankem, RFCL Limited, New Delhi, India), MgO (Merck Specialties India Limited, Mumbai, India) and Ethanol (Changshu Yangyuan Chemical Cooperation Limited, China) were received and used as such for the synthesis of catalyst nanoparticles. Carbon precursors like ferrocene and xylene (Merck Specialties India Limited, Mumbai, India) were received and used as such for synthesis of CNTs by CVD method. Argon gas (Bhandari Carbonic, Jalgaon, India) was used as carrier and inert gas. Nitric acid-HNO_3 (S.D. Fine-Chem limited, Mumbai, India) was used for purification of CNTs. Sulphuric acid (H_2SO_4) and potassium dichromate (K_2CrO_7) were also received for cleansing treatment of glass slides. Aniline and ammonium persulphate-APS (Fisher Scientific, Mumbai, India) was received and used as such for the preparation of nanostructured PAni. Sodium dodecyl sulphate (SDS), hydrochloric acid (HCl) and perchloric acid ($HClO_4$) were procured from (Himedia Laboratories Private Limited, Mumbai, India), while *N*-methyl-2-pyrrolidone (NMP) was received from (Merck Specialities India Limited, Mumbai, India). Anhydrous ferric chloride ($FeCl_3$) and sodium hydroxide (NaOH) were purchased from (RFCL Limited, Mumbai, India) and methanol was received from (S.D. Fine-Chem Limited, Mumbai, India). Ultra-pure demineralised (DM) water 18 (MΩ) was prepared in Smart2Pure system (Thermo Electron LED GmbH, Germany) and used for the preparation of various solutions and washing purposes. Cotton thread, Grifin 40 (Madura Coats Private Limited, Bangalore, India) was used as a stretchable material to prepare conductive cotton threads. Commercial LPG gas (for cooking purpose) was used to study sensing performance of multigrade hybrid nanostructured conductive threads.

2.2 Synthesis of catalyst nanoparticles.

Catalyst nanoparticles of Fe/MgO were synthesized in an autoclave reactor by hydrothermal method which resulted particles at nanoscale with high specific surface area and active sites. These nanofabricated catalysts were used to synthesize CNTs with good % yield. Details of steps involved for the preparation of Fe/MgO catalyst nanoparticles (K1, K2 and K3) are discussed in section S2 of supplementary information, while Figure S1 shows its schematic. Table 1 shows composition of reactants taken for synthesis of Fe/MgO catalyst nanoparticles.

2.3 Synthesis and purification of CNTs.

CNTs were synthesized using CVD reactor setup which was designed and supplied by (Lelesil Innovative System, Mumbai, India). Construction, design and working of CVD reactor setup are discussed in section S3 of supplementary information. Figure S2 illustrates detail design of CVD set up, while Table S1(a-c) shows its dimensions. Detail of steps for synthesis of CNTs by CVD method is discussed in section S4 of supplementary information. Figure S3(a) illustrates arrangement of CVD reactor set up, while Figure S3(b) shows graphical presentation of steps involved in synthesis of CNTs by CVD method using carbon precursors. Graphical steps indicates that preheating and cooling periods were kept of 20 min, while vapor deposition/residential time was kept 20-40 min during which CNT growth took place at temperature range between 800-1000 ^{o}C. The resulting materials were soft and spongy in nature with a carbonaceous texture indicating the vicinity of CNTs.

Purification of CNTs was achieved by number of strategical steps (in section S5 of supplementary information), which involves extraction of impurities, oxidation and acid treatment, separation and drying as shown in Figure 1. The method was comprised of (i) evacuation of soluble impurities using solvent (e.g. toluene), (ii) liquid-phase oxidation of amorphous carbon, (iii) an acid treatment for removal of unprotected metallic catalyst

particles, (iv) ultracentrifugation step for separation of the CNTs from the unwanted graphitic impurities and protected catalysts and (v) drying to obtain powdered material. This intriguing method is exceptionally useful because it allows for the selective extraction of impurities from CNT samples.

2.4 Synthesis of PAni/γ-Fe_2O_3 nanostructures.

Synthesis of γ-Fe_2O_3 nanoparticles was carried out as per earlier approach [1] of ultrasound cavitation steps as shown in Figure 2(a). PAni/γ-Fe_2O_3 nanostructures were also prepared by previous approach [1] of *in-situ* chemical polymerization as shown in Figure 2(b). The microscope glass slides (Polar India Corporation, Mumbai) were used for observation of PAni/γ-Fe_2O_3 nanostructures. These glass slides were cleaned by keeping in chromic acid-H_2CrO_4 (mixture of H_2SO_4 and K_2CrO_7) solution for 30 min. Finally, these clean slides were allowed to immerse completely in 0.1M HCl solution for 60 min. The slides were then progressively sonicated in water and methanol for 15 min each, followed by vacuum drying prior to use for analysis of PAni/γ-Fe_2O_3 nanostructures.

2.5 Preparation of hybrid nanostructured cotton threads.

2.5.1 Cleaning treatment and functionalization of the cotton threads using CNT ink. A commercial white cotton thread was used to prepare nanostructured sensing threads. At first, threads were washed with hot water. Since the surfaces of threads are fibrous, they were also allowed to treat with an ethanol which eliminated the redundant fibres. Threads were also cleaned three times by acetone and DM water. These clean threads were immersed into 5M HNO_3 solution for 60 min to increase the hydrophilicity. Finally, threads were rinsed with DM water by providing ultrasound effect for 15 min and dried in an oven for 15 min to remove water traces. Pure CNTs were uniformly incorporated onto the surface of cotton

thread using well-dispersed CNTs' colloidal solution. First, CNTs were treated with 5M HNO_3 for 30 min and then with 40 mg/mL of SDS, which finally were dispersed in DM water. Last, the colloidal mixture of CNT was sonicated for 20 min before functionalizing them on the surface of cotton threads. The pure cotton threads were alternately dipped into the colloidal solution of CNT ink. Finally, the mixture was sonicated for 20 min. Due to the hierarchical and permeable structure of cotton thread; it quickly swells the large amounts of the CNT from colloidal solution [23,25,61-64,71-72]. The conductive cotton threads were dried in an oven at 80 ^{o}C for 120 min.

2.5.2 Incorporation of PAni/γ-Fe_2O_3 nanostructures on conductive threads using strategical protocol. Conductive (CNTs functionalized) cotton threads were immersed in solution of *in-situ* polymerized PAni/γ-Fe_2O_3 nanostructures and then uniformly mixed for 15 min under ultrasound environment. Then it was allowed to stir continuously for 12 hr and left to stand overnight. These hybrid nanostructured conductive cotton threads were dried in an oven at 80 ^{o}C for 2 hr. Table 2 shows the quantity and size of materials and reactants taken during preparation of hybrid nanostructured cotton threads. Before being used for the first time, each thread sample was dipped in solution and allowed to treat for 15 min under ultrasound effect for uniform distribution of multigraded nanostructures. Subsequently their reinforcement on each cotton thread was carried out successfully under ultrasound environment.

2.6 Characterization and measurement techniques.

2.6.1 X-ray diffraction (XRD). An XRD analysis of nanofabricated catalyst particles, CNTs, γ-Fe_2O_3 nanoparticles and PAni/γ-Fe_2O_3 nanostructured composite was conducted on an Advance X-ray diffractometer, (D8, Brukers Germany) with $CuK\alpha_1$ radiation (λ = 1.5404 Å) within the 2θ range of 20-80 ^{0}.

2.6.2 Field emission-scanning electron microscopy (FE-SEM). FE-SEM (S-4800, Hitachi, Tokyo, Japan) microscope was used to study growth mechanism of CNTs, size and shape of γ-Fe_2O_3 nanoparticles and surface morphology of PAni/γ-Fe_2O_3 nanostructured composites and multigraded nanostructured threads. The CNTs were dispersed in acetone and subjected to ultrasound treatment for 10 min to obtain a holey carbon film before viewing under the microscope. Hybrid nanostructured cotton threads were gold coated and mounted on specimen tub prior to view in microscope.

2.6.3 Tunneling electron microscopy (TEM). The exact size and shape of MWCNTs were studied by CM200, TEM (Philips, Netherlands) at a resolution of 2.4 Å and operating voltage of 20–200 kV. Pure MWCNTs were dispersed in water and kept in conventional ultrasonic bath for 10 min. This sonicated crude droplet of colloidal suspension was dried and then put on holey electron micro copper grid of microscope specimen.

2.6.4 Current-voltage (I-V) measurements by four probe conductivity meter. The Current-voltage (I-V) characteristic values of nanostructured threads were measured by four-point probe conductivity meter, using a current source (CCS-01) and micro voltmeter (DMV-001, SES Instruments, Scientific Equipments, Roorkee, India). Each sample of nanostructured thread was placed in contact with four-probes and variation in an electrical current was studied. The voltage was applied, at same time current was recorded in the bias range of 2 to −2 V by a multi meter using four probes. All the electrical measurements were carried out at an ambient temperature 30 ± 2 ^{o}C. The (I–V) characteristic values of each thread sample were recorded in the presence of air at ambient temperature. The conductive/ohmic nature of nanostructured thread was studied from (I–V) characteristic graphs.

2.6.5 Gas sensing procedure and characteristic properties. Figure 3 shows schematic representation of two probe gas sensing setup, while actual arrangement of set up at

laboratory is shown in Figure S4. Construction details of set up are described in section S6 of supplementary information. Gas sensing experiments were carried in a sealed quartz glass test chamber (Vijay Scientifics, Aurangabad, India) of 1.5 L volume as shown in Figure S4. The samples of hybrid nanostructured cotton threads were attached on glass substrate and both ends were contacted between two conducting probes. At first, chamber was evacuated and purged continuously with pure argon gas. Then, 50 ppm of commercial grade (household purpose) LPG gas was injected using syringe into the glass chamber. Both ends of nanostructured cotton threads were contacted with help of two probes connected to programmable 4.5 digital multimeter (SM 5015, Scientific MES-Technik Private Limited, Indore, India). This multimeter was attached to a computer (QT035AV, Hewlett Packard, Banglore, India) using a RS232C interface that was fully automated and logged by a program. The (I–V) characteristic values were recorded in the bias range of 0.15 to −0.15 V at interval of 1 sec. A change in current was deduced from (I–V) characteristic plot; and gas response value was calculated from a change in current and current measured in the presence of air. The response of the sensor was calculated from (I–V) characteristics. All the (I–V) characteristic values were measured at an ambient temperature (30±2 ^{o}C) in the presence of air as well as 50 ppm of LPG. Equation (1) shows gas response (R_{resp}) value which is defined as the ratio of change in current to the current of sensing thread measured in the vicinity of air.

$$R_{resp} = \left(\frac{I_g - I_a}{I_a} \right) = \left(\frac{\Delta I}{I_a} \right) \qquad (1)$$

In equation (1), I_g is current of sensing thread measured on exposure of LPG gas, while I_a is current of sensing thread measured in the presence of air, and ΔI is the change in current. Response time (t_{resp}) is defined as the time needed for a sensor to attain the 90% of change in

current on exposure of test gas, while recovery time (t_{reco}) is defined as the time taken by sample to get back 90% of original current in vicinity of the air. The selectivity is defined as ability of optimum value of nanostructures in sensing threads to respond to a certain ppm of gas, while in earlier work selectivity is defined with respect to particular gas [9,14]. The response and recovery time periods of the junction were determined by holding the junction to potential range (0.15 to −0.15 V) and recording current with respect to time [3-4].

3 Results and discussions

3.1 Crystallinity studies.

3.1.1 Crystalline behavior of catalyst nanoparticles. XRD patterns of the nanofabricated Fe/MgO catalyst particles are shown in Figure 4. Nanoparticles of Fe/MgO catalyst exhibit characteristic peaks of MgO support and oxides of Fe metal. The crystal planes for MgO was observed at (2 2 0), which is at a distance from main peak of Fe (1 0 0) in Figure 4. The peak observed at $2\theta = 43^0$ was assigned to Fe (1 0 0) plane, while peak at $2\theta = 67^0$ was allocated to MgO (2 2 0).

3.1.2 Crystalline nature of CNTs. Figure 5 also shows X-ray diffractograms of the CNTs grown over the catalyst K1, K2, and K3. The XRD pattern clearly shows that the CNTs were pure and well graphitized. The entire XRD pattern of CNTs shows four major peaks at $2\theta = 26^0$, 44^0, 56^0 and 62^0 for all catalyst obtained from Fe/MgO. The respective graphite like reflections at above primary peaks (0 0 2), (1 0 0), (0 0 4), and (1 1 0) for all samples. The peak at $2\theta = 26^0$ confirms the presence of more crystalline graphitic carbon in the CNTs synthesized by all catalyst K1 and K3. It is observed that peak for catalyst K2 is slightly visible at $2\theta = 26^0$. Table 3 shows yield and crystallinity of CNT synthesized using different catalyst K1, K2 and K3. When CNTs was synthesized using catalyst K2, greater crystallinity

was observed relative to those synthesized using catalyst K1 and K3 owing to their different electronic structure.

3.1.3 Crystal structure of γ-Fe_2O_3 nanoparticles and PAni/γ-Fe_2O_3 nanocomposites. X-ray diffractograms of PANi and its nanocomposites were studied earlier [1]. From observed peaks and d-values in the range of 0.12-0.30 nm, it is confirmed that γ-Fe_2O_3 nanoparticles were cubic [1]. The crystallite size of these γ-Fe_2O_3 nanoparticles was calculated by Scherrer's equation, and was found to be 29.5 nm, while the crystallinity was 55 %. The crystallinity of PAni/γ-Fe_2O_3 (3 wt%) nanostructures was reported to be 63 % [1].

3.2 Surface morphology.

3.2.1 Shape and size of catalyst nanoparticles. Figure 4 shows FE-SEM micrographs indicating size, shape and definite crystalline morphology of nanofabricated catalyst particles. It can be seen from Figure 4 that the catalyst particles possess nano-spherical shape with smooth surface. The size of K1 catalyst nanoparticle was reported to be 33-67 nm and size of K3 catalyst nanoparticle was observed to be small of 5.5-14 nm. Uniform particles size was observed in the case of K2 catalyst nanoparticles, which also shows increment in % yield of CNT produced.

3.2.2 Growth and morphology of CNTs. Growth of CNTs was observed at different temperatures ranging from 500 to 1000 ^oC, which is shown in Figure S5(a-e) and discussed in section S7 of supplementary information. TEM and FE-SEM cross-section micrograph in Figure 5(a) shows growth of MWCNTs at 900 ^oC using K2 catalyst after chemical vapor deposition time of 20 min. Figure 5(a) demonstrates that MWCNTs having small diameters might be exist at 1000 ^oC or even SWCNTs. In general, CNTs grow on catalyst nanoparticles and might have almost smaller or similar diameter to catalyst nanoparticles. These results are in close agreement with the consequences of XRD patterns which are demonstrated and

discussed in earlier section. TEM micrograph in Figure 5 shows multiwall of CNTs. TEM study reveal that most of multi-layered CNTs were having diameter in the range 30-5 nm. Hence the MWCNTs are crystalline in nature with least defect due to effect of ultrasonication and centrifugation steps during purification [28].

3.2.3 Nanostructures of PAni/γ-Fe_2O_3 composites. Figure 6(a-b) elaborates the FE-SEM micrographs of γ-Fe_2O_3 nanoparticles and PAni/γ-Fe_2O_3 (3 wt%) nanocomposites. Uniform, nanofibers of PAni/γ-Fe_2O_3 (indicated by blue arrows) with a diameter of ~72 nm was observed in Figure 6(a). This shows the adequacy of ultrasound in producing non-aggregated nanofibres in the absence of an encapsulating agent. Figure 6(b) shows the uniform dispersion of γ-Fe_2O_3 nanospheres (indicated by white circles) in the PAni matrix. Nanofibrillar morphology of PAni having diameter of about 70-74 nm can be clearly seen. It appears that increasing the amount of γ-Fe_2O_3 nanoparticles can result [1] larger diameter of PAni nanofibers. From the FE-SEM results as shown in Figure 6(b), it is evident that ultrasound induced cavitation can produce non-aggregated, nanostructured γ-Fe_2O_3 particles, and also it can aid uniform dispersion of the nanoparticles into the polymer matrix.

3.2.4 Hybrid nanostructured surface of conductive cotton threads. Figure 7 shows schematic, graphical and actual FE-SEM views of hybrid nanostructured conductive threads. Schematic view in Figure 7 indicates that CNTs were successfully incorporated in to individual micro fibrils of cotton threads. Graphical view of the Figure 7 demonstrates that as electrical conductivity increases as mass loading of CNT increases. The amount of CNTs coating can be easily controlled by changing the concentration of CNT ink and dipping time. Considering mechanical flexibility and strength for the conductive threads, it is not preferred to increase the mass loading of CNTs [64].

Genuine photographic FE-SEM view in Figure 7 shows that flexible cotton threads coated with various loading of CNTs. Incorporated CNT/PAni/γ-Fe_2O_3 (3 wt%) hybrid

nanostructures (red circles) can be visualized on the surface of cotton threads (green arrows) as shown in FE-SEM view of Figure 7.

Figure 8(a-f) shows FE-SEM micrographs indicating presence of PAni/γ-Fe_2O_3 nanostructures on conductive cotton threads. Due to ultrasound effect, PAni/γ-Fe_2O_3 nanostructures get uniformly distributed over the surface of conductive threads without aggravating its diameter and length. It can be said that when amount of γ-Fe_2O_3 nanoparticles was increased, embedment of PAni/γ-Fe_2O_3 nanostructures was resulted with larger diameter. The blue coloured circle area shows the vicinity of PAni/γ-Fe_2O_3 nanostructures on surface of conductive threads and it was also reported that increasing the amount of PAni/γ-Fe_2O_3 nanostructures can lead effective sensing and response [1]. LPG sensing response of hybrid nanostructured conductive thread can be increased by increasing the amount both of CNT as well as PAni/γ-Fe_2O_3 nanostructures. The large surface area of γ-Fe_2O_3 nanoparticles can adequately provide greater adsorption sites for detection of gas molecules which may enhance response at higher γ-Fe_2O_3 nanoparticles content. On another hand increase in loading of CNT provides high conductivity and strength to the cotton thread. Figure 9(a-b) clearly shows loading of PAni/γ-Fe_2O_3 (3 wt%) nanostructures incorporated at different wt%. Green circles shows evidence of CNTs functionalized on cotton threads (blue arrows) shown in Figure 9(c).

3.3 Electrical (I–V) characteristics of hybrid nanostructured cotton threads.

Figure 10(a-c) illustrates (I–V) characteristics of conductive cotton threads functionalized by CNT as well as PAni/γ-Fe_2O_3 nanostructures. Earlier, semi conducting nature of PAni/γ-Fe_2O_3 nanocomposites was reported from the non-linear nature of (I–V) characteristics [1]. In Figure 10(a) shows (I–V) characteristics of pure thread, Figure 10(b) shows effect of various CNT loadings and Figure 10(c) shows effect of various loading of PAni/γ-Fe_2O_3

nanostructure on (I–V) characteristics. It is clear from all symmetrical (I–V) characteristics that the electrical contacts on the films can show ohmic nature. CNT exhibits higher electrical conductivity than that of PAni/γ-Fe_2O_3 nanostructures as shown in Figure 10(a) and here both shows linear nature. Higher electrical conductivity of thread was observed on increasing the amount of CNT content nanostructures and can be confirmed from Figure 10(b), while PAni/γ-Fe_2O_3 nanostructures loadings may decrease the electrical conductivity and this can be confirmed from nanostructures as shown in Figure 10(c). Meanwhile, Figure 10(b-c) shows the current-voltage (I–V) characteristics of hybrid nanostructured threads.

3.4 Gas sensing performance of hybrid nanostructured cotton threads.

3.4.1 Gas sensing characteristics. Figure 11(a-e) illustrates gas sensing characteristics of hybrid nanostructured threads which can detect 50 ppm LPG at ambient temperature. Conducting nature of PAni/γ-Fe_2O_3 nanocomposite was confirmed because of adsorption of LPG molecules. As shown in Figure 11(a), no significant change in electrical resistance when conductive thread was observed was exposed to LPG, *i.e.* conductive threads do not render the sensing response value to LPG as compared to PAni/γ-Fe_2O_3 nanostructures. PAni/γ-Fe_2O_3 nanostructures showed a significant reduction in current due to the adsorption of LPG molecules over their surface and also PAni/γ-Fe_2O_3 nanocomposites were semiconducting in nature [1]. However, with the incorporation of γ-Fe_2O_3 nanoparticles can pronounce increment in resistance of PAni/γ-Fe_2O_3 nanocomposite when exposed to low concentration (50 ppm) of LPG. This increment in resistance on exposure to LPG becomes more significant with increasing content of γ-Fe_2O_3 nanoparticles [1].

3.4.2 Selectivity of composition. Figure 11(b-c) depicts the current-time characteristics indicating the variation in loading of CNT and PAni/γ-Fe_2O_3 nanostructures over the surface of cotton threads. Figure 11(b) shows current-time characteristics of sensing threads

incorporated with various loading of CNT by keeping constant loading of PAni/γ-Fe_2O_3 nanostructures. Figure 11(b) also shows that selective composition of CNT/(PAni/γ-Fe_2O_3) nanostructures loading was 75/75. Similarly Figure 11(c) shows current-time characteristics of hybrid nanostructured thread incorporated with various loading of PAni/γ-Fe_2O_3 nanostructures by keeping constant loading of CNTs. Selective and optimum composition ratio of CNT/(PAni/γ-Fe_2O_3) nanostructures loading was 100/125. Optimum and selective loading of CNT shows better sensing response towards LPG detection owing to higher loading of CNTS, superior conductivity of CNT and higher loading of PAni/γ-Fe_2O_3 nanostructures. It is clear from the characteristics that both optimum and selective composition ratio of CNT/(PAni/γ-Fe_2O_3) nanostructures at 100/125 was selective ratio for hybrid nanostructured sensing threads for detection of 50 ppm LPG.

3.4.3 Response and recovery times. A very short, i.e., quick response time (t_{resp}) of hybrid nanostructured conductive threads should be understood in the framework of rapid gas diffusion over sensing surface due to the nano porous shell structures. This obviously confirms that the multigrade hybrid CNT/(PAni/γ-Fe_2O_3) nanostructures are promising materials for the development of highly sensitive and fast responding gas sensor. As shown in Figure 11(d-e), the response time (t_{resp}) of hybrid nanostructured sensing threads was observed to be ~20-25 sec and the minimum recuperation/recovery time (t_{reco}) was observed to be ~35-40 sec. It can be said that hybrid nanostructured sensing threads showed quick response and fast recovery time, which may be due to its crystalline nature, nanoscale morphology, high LPG adsorption capability on the expansive surface of γ-Fe_2O_3 activator molecules and therefore fast reduction of exposed gas.

3.4.4 Gas sensing response value. Figure 12(a-b) shows sensing response values for detection of LPG by hybrid nanostructured threads on variation in loading of both CNT and (PAni/γ-Fe_2O_3) nanostructures. The sensing threads loaded with CNT/PAni/γ-Fe_2O_3

(100/125) nanostructures were observed to be highly sensitive towards detection of LPG. LPG sensing response value of hybrid conductive threads loaded with CNT/PAni/γ-Fe_2O_3 (100/125) nanostructures showed a highest response (R_{resp}= 0.91) value at an ambient temperature as compared to other samples. A high response value towards LPG detection may be due to the uniform dispersion of γ-Fe_2O_3 activator molecules and CNTs with nanoscale morphology over the surface of cotton threads which enable thread to enhance the capacity of adsorption of gas molecules. This γ-Fe_2O_3 activator molecules with nanoscale morphology might be responsible for higher reactivity of PAni/γ-Fe_2O_3 nanocomposites with LPG molecules. Notwithstanding this, multi-microstructures (associated with nanoparticles and nanostructures spheres, uniformly distributed fine hillocks of γ-Fe_2O_3 particles) would also be responsible for high sensing response [1]. Table 4 shows the comparison between LPG sensing performance of hybrid nanostructured threads prepared in this currently reported work and that of previously reported work by our group [1] as well as by other reported work using simple nanocomposites. It is noteworthy that the multigrade nanostructured sensing threads prepared in currently reported work exhibits better sensing response (R_{resp} = 0.91), quick response time (~20-25 sec) and fast recovery time (~35-40 sec) as compared to those reported in all previous work. Patil et al [2] also summarized various LPG sensors for detection of different ppm of LPG at higher temperature (> 150 ^oC). Singh et al [17] also compared and summarized various sensors for LPG detection showing sensing performance at room temperature. At higher temperature these multigrade nanostructured sensing materials could be a ideal candidate for LPG gas detection because of their better thermal stability as shown in Figure S6 and discussed in section S8 of supplementary information.

3.4.5 LPG sensing phenomena and reaction mechanism. The LPG sensing mechanism of sensor is a surface controlled phenomenon i.e., it is based on the surface area of the nanostructured materials. Initially, oxygen from the atmosphere gets adsorbed on the surface

of the film and pick up electrons from its conduction band. The sensitivity of a sensor is mainly determined by the interactions between the gases and the surface of a sensor. The enhanced sensitivity of the hybrid nanostructured threads based sensor may be attributed to its surface related factors (1D surface morphological structure); such as high surface area, a large space charge layer change and small crystallite size. The specific surface area of nanocrystallites is larger. Further, the small crystallites of γ-Fe_2O_3 provide more adsorption–desorption sites, as a result of the increased amounts of surface atoms and grain boundaries, which will also give a contribution to increment in the sensitivity of the sensor [1,17]. It is already demonstrated in previous work [1] that response value was 0.5 for detection of 50 ppm LPG and it was 1.3 for detection of 200 ppm LPG. In this research work, gas response value of hybrid nanostructured is reported 0.91 for detecting the low concentration (50 ppm) of LPG. Therefore, larger number of LPG molecules could be adsorbed so higher gas response is possible.

In fact, during adsorption of gas molecules on the surface of thread, a potential barrier to charge transport is developed. This may significantly increase concentration of electrons due to sensing phenomena, which promotes an increment in sensor's response. Also, the adsorption of gas molecules depends on distribution of hybrid nanostructures over the surface of threads. The LPG sensing response of multigrade nanostructured thread is restricted by the speed of the chemical reaction because the gas molecules have enough thermal energy to react with the surface (Figure 13). High sensing of LPG molecules may be due to nanospherical γ-Fe_2O_3 particles uniformly distributed on the surface of CNT functionalized conductive thread. Adsorption of LPG molecules plays a vital role in the electrical and sensing properties of hybrid nanostructured thread. An adsorption of LPG molecules removes the conduction electrons and enhances the resistance of thread sensor. The LPG molecule is

conceivably converted at iron oxide surface (in presence of adsorbed oxygen ions) by dehydration reaction [2] as shown below.

$$C_nH_{2n+2} + 2O^- \rightarrow H_2O + C_nH_{2n}{:}\,O + e^- \text{ (dehydration)}$$

Here, LPG (C_nH_{2n+2}) represents CH_4, C_3H_8, C_4H_{10}, while C_nH_{2n}:O molecules which are partially oxidized intermediates on the surface of γ-Fe_2O_3 nanospheres. Thus, during oxidizing phenomena, LPG molecule generally liberates electrons into the conduction band. This addition of electron into the conduction band of sensing surface on threads is result of decreases in resistance of the sensor [13,19]. As it is already discussed earlier [1] that PAni/γ-Fe_2O_3 nanostructures show high sensing response to LPG gas due to the presence of adsorption centre of Fe(III). Moreover, high dispersity of PAni/γ-Fe_2O_3 nanostructures on the conductive threads provides efficient electron exchange between the cations: Fe (III) ↔ Fe(II). All this produces more prominent conductivity drop of the active layer and consequently enhances the sensor performance.

4 Conclusions

In summary, flexible conductive cotton threads were used as a platform to prepare a cable-type hybrid nanostructured sensor using CNTs and PAni/γ-Fe_2O_3 multi-grade nanostructures via facile strategical synthesis under ultrasound environment. The study shows that CNTs were optimally grown on Fe/MgO nanoparticles (10-60 nm) by CVD method at 900 ^oC and purified using the combination of several chemical methods. On another hand, sonochemically synthesized γ–Fe_2O_3 nanoparticles (3 wt%) were decorated and found to be disseminated uniformly into the *in-situ* polymerized nanofibrous PAni matrix (60-75 nm) due to effect of ultrasound which leads to in ion. These hybrid nanostructures were successfully

incorporated over the surface of the conductive cotton threads which were then investigated for LPG detection at an ambient temperature. The response values were found to be increased with increasing amount of CNTs. The large surface area of γ-Fe_2O_3 nanoparticle provides greater adsorption sites for the gas molecules, which resulted in high sensing response value. The interaction between the gas molecules and the hybrid nanostructures induces a potential causing an increase in the depletion area of PAni/γ-Fe_2O_3 nanostructures. As a result, the resistance of hybrid nanostructured thread increases upon exposure to LPG molecules. The nanoscale morphology of hybrid conductive threads gives an expansive surface for adsorption of gas molecules which enhances gas response value. High response values of multigrade hybrid nanostructured thread may be due to the combined effects of (i) Low Fe-O bonding energy and smaller electro negativity, (ii) presence of nanostructured γ-Fe_2O_3spheres and (iii) high adsorption capability of gas.

These cable type flexible sensors of multi-grade dynamic nanostructures of CNT/PAni/γ-Fe_2O_3 functionalized threads can be useful in the development of wearable sensing device at an ambient temperature. Here, it is offered a uniquely simple yet remarkably functional solution for the development of wearable smart textiles, with considering many parameters exceeding the existence of technological solutions, including those using carbon materials. One of the most attractive features of this approach is the simple steps involved in both the preparation and operation of the sensor. Furthermore, since a commodity such as cotton is used as a substrate and the CNT used in a very low amount, mass production of disposable wearable sensors should be conceivable. From the technological point of view, sensors could be integrated in connection with wearable data-reading devices owing to their conductive nature. The as-made hybrid nanostructured cotton threads are flexible and robust enough to be intertwined, knotted and woven in a cloth and making the smart garment possible. And this highly bendable cloth based sensor can be woven from cm-long coaxial fibres, promising

the application in next generation of smart, safe and flexible garment devices or intelligent sensors.

Acknowledgement

Authors are thankful to Council of Scientific and Industrial Research (CSIR), New Delhi, India (Project no.: 02(0023)/11/EMR–II) for providing financial assistance to carry out the major research project. Authors are also thankful to Dr. Tanushree Sen for providing samples of polymer nanocomposites and necessary guidance. The authors (D.P. Hansora and R. Yadav) have contributed equally as first authors in this manuscript.

References

1. T. Sen, N.G. Shimpi, S. Mishra and R. Sharma, *Sens. Actuator B,* 2014, **190**, 120-126. http://dx.doi.org/10.1016/j.snb.2013.07.091
2. L.A. Patil, M.D. Shinde, A.R. Bari, V.V. Deo, D.M. Patil and M.P. Kaushik, *Sens. Actuators B,* 2011, **155**, 174-182. http://dx.doi.org/10.1016/j.snb.2010.11.043
3. D.S. Dhawale, D.P. Dubal, V.S. Jamadade, R.R. Salunkhe, S.S. Joshi and C.D. Lokhande, *Sens. Actuators B,* 2010, **145,** 205–210. http://dx.doi.org/10.1016/j.snb.2009.11.063
4. D.S. Dhawale, R.R. Salunkhe, U.M. Patil, K.V. Gurav, A.M. More and C.D. Lokhande, *Sens. Actuators B,* 2008, **134**, 988–992. http://dx.doi.org/10.1016/j.snb.2008.07.003
5. D.S. Dhawale, R.R. Salunkhe, V.J. Fulari, M.C. Rath, S.N. Sawantc and C.D. Lokhande, *Sens. Actuators B*, 2009, **141,** 58–64. http://dx.doi.org/10.1016/j.snb.2009.06.025

6. K.R. Nemade and S.A. Waghuley, *J. Mater. Sci. Eng. B,* 2013, **3(5),** 310-313. http://www.davidpublishing.com/davidpublishing/Upfile/8/19/2013/2013081906899848.pdf

7. S.B. Kulkarni, B.B. Raje Shaikh, C.D. Lokhande and S.S. Joshi, *J. Shivaji Univ., Sci. Technol.,* 2014, **41(2),** 1-2. ISSN-Science-0250-5347.

8. S. Sarkar and D. Basak, *Sens. Actuators B,* 2013, **176**, 374–378. http://dx.doi.org/10.1016/j.snb.2012.10.095

9. S.S. Barkade, D.V. Pinjari, U.T. Nakate, A.K. Singh, P.R. Gogate, J.B. Naik, S.H. Sonawane and A.B. Pandit, *Chem. Eng. Proc.,* 2013, **74,** 115–123. http://dx.doi.org/10.1016/j.cep.2013.09.005

10. B.A. Bhanvase, N.S. Darda, N.C. Veerkar, A.S. Shende, S.R. Satpute and S.H. Sonawane, *Ultrason. Sonochem.,* 2014. http://dx.doi.org/10.1016/j.ultsonch.2014.11.009

11. R.B. Birajadara, A. Ghosh, A. Ghule, F. Singh and R. Sharma, *Sens. Actuators B,* 2011, **160**, 1050–1055. http://dx.doi.org/10.1016/10.1016/j.snb.2011.09.024

12. S.S. Joshi, C.D. Lokhand and S.H. Han, *Sens. Actuators B,* 2007, **123,** 240–245. http://dx.doi.org/10.1016/j.snb.2006.08.023

13. K.R. Nemade, R.V. Barde and S.A. Waghuley, *J. Taibah Univ. Sci.,* 2015. http://dx.doi.org/10.1016/j.jtusci.2015.03.003

14. P.T. Patil, R.S. Anwane and S.B. Kondawar, *Proc. Mater. Sci.,* 2015, **10,** 195–204. http://dx.doi.org/10.1016/j.mspro.2015.06.041

15. Y.T. Ravikiran, S. Kotresh, S.C. Vijayakumari and S. Thomas, *Curr. Appl. Phys.,* 2014. http://dx.doi.org/10.1016/j.cap.2014.04.015

16. S. Singh, M. Singh, B.C. Yadav, P. Tandon, S.I. Pomogailo, G.I. Dzhardimalieva and A.D. Pomogailo, *Sens. Actuators B,* 2011, **160,** 826–834.

http://dx.doi.org/10.1016/j.snb.2011.08.068

17. A. Singh, A. Singh, S. Singh, P. Tandon, B.C. Yadav and R.R. Yadav, *J. Alloys Compounds,* 2015, **618**, 475–483. http://dx.doi.org/10.1016/j.jallcom.2014.08.190
18. N.B. Sonawane, K.V. Gurav, R.R. Ahire, J.H. Kim and B.R. Sankapale, *Sens. Actuators A,* 2014, **216,** 78–83. http://dx.doi.org/10.1016/j.sna.2014.05.012
19. V.R. Shinde, T.P. Gujar and C.D. Lokhande, *Sens. Actuators B,* 2007, **123,** 701–706. http://dx.doi.org/10.1016/j.snb.2006.10.003
20. K.V. Gurav, P.R. Deshmukh and C.D. Lokhande, *Sens. Actuators B*, 2011, **151,** 365−369. http://dx.doi.org/10.1016/j.snb.2010.08.012
21. G. Sberveglieri, *Sens. Actuators, B* 1995, **23**, 103-109. http://dx.doi.org/10.1016/0925-4005(94)01278-P
22. X. Liu, S. Cheng, H. Liu, S. Hu, D. Zhang and H. Ning, *Sens.,* 2012, **12**, 9635-9665. http://dx.doi.org/10.3390/s120709635
23. J.W. Han, B. Kim, J. Li and M. Meyyappan, *Appl. Phys. Lett.,* 2013, **102**, 1-4. http://dx.doi.org/10.1063/1.4805025
24. T. Guinovart, M. Parrilla, G.A. Crespo, F.X. Rius and F.J. Andrade, *Anal.,* 2013, **138**, 5208-5215. http://dx.doi.org/10.1039/c3an00710c
25. L.M. Castano and A.B. Flatau, *Smart Mater. Struct.* 2014, **23**, 1-27. http://dx.doi.org/10.1088/0964-1726/23/5/053001
26. S. Mishra, N.G. Shimpi and T. Sen, *J. Polym. Res.,* 2013, **20**, 49. http://dx.doi.org/10.1007/s10965-012-0049-5

27. N.G. Shimpi, S. Mishra, D.P. Hansora, U. Savdekar, *Indian Patent* 3179/MUM/2013 (2013). http://ipindia.nic.in/ipr/patent/journal_archieve/journal_2013/pat_arch_102013/official_journal_25102013_part_i.pdf

28. D.P. Hansora, N.G. Shimpi, and S. Mishra, *JOM,* 2015. http://dx.doi.org/10.1007/s11837-015-1522-5

29. V.N. Popov, *Mater. Sci. Eng. R,* 2004, **43**, 61-102. http://dx.doi.org/10.1016/j.mser.2003.10.001

30. B. Mahar, C. Laslau, R. Yip and Y. Sun, *IEEE Sens. J.,* 2007, **7**, 266-284. http://dx.doi.org/10.1109/JSEN.2006.886863

31. H. Dai, *Surf. Sci.,* 2002, **500**, 218-241. http://dx.doi.org/10.1016/S0039-6028(01)01558-8

32. K. Matzinger, *Ph.D. Theses*, Universität Freiburg, 2006. https://doc.rero.ch/record/6666/files/MatzingerK.pdf

33. N. Gupta, S. Sharma, I.A. Mir and D. Kumar, *J. Sci. Ind. Res.,* 2006, **65**, 549-557. http://nopr.niscair.res.in/bitstream/123456789/4862/1/JSIR%2065(7)%20549-557.pdf

34. B. Crawford, D. Esposito, V. Jain, D. Pelletier, C. Mavroidis, Y.J. Jung and A. Khanicheh, Paper 55, *Mechanical Engineering Undergraduate Capstone Projects,* Final Report, Northeastern University, 2007. http://iris.lib.neu.edu/cgi/viewcontent.cgi?article=1054&context=mech_eng_capstone

35. A. Abbaspourrad, C. Verissimo, R.V. Gelamo, M.M. Silva, A.R. Vaz, F.P.M. Rouxinol, O.L. Alves and S.A. Moshkalev, *Smart Nanocompos.*, **1**, 13-18. https://www.novapublishers.com/catalog/product_info.php?products_id=25809

36. M. Ding, *Ph.D. Theses,* University of Pittsburgh, 2013. http://d-scholarship.pitt.edu/19257/4/Mengning_Ding_ETD_2013.pdf

37. Z. Chen and K. Saito, *UCR Review Meeting*, University of Kentucky, 2007. http://seca.doe.gov/publications/proceedings/05/UCR_HBCU/pdf/papers/Zhi_Chen.pdf

38. M.D. Volder, D. Reynaerts and C.V. Hoof, *Proceeding of the Conference on IEEE Sensors*, 2010, 2369-2372. http://mechanosynthesis.mit.edu/conferences/026_devolder_sensors10_bridgetempsensor.pdf

39. E. Llobet, *Sens. Actuators B,* 2013, **179**, 32-45. http://dx.doi.org/10.1016/j.snb.2012.11.014

40. A. Misra, S*pecial section: Carbon Technology, Curr. Sci.,* 2014, **107**, 419-429. www.currentscience.ac.in/Volumes/107/03/0419.pdf

41. J. Wang and M. Musameh, *Anal.,* 2004, **129**, 1-2. http://dx.doi.org/10.1039/b313431h

42. D. Jariwala, V.K. Sangwan, L.J. Lauhon, T.J. Marksa and M.C. Hersam, *Chem. Soc. Rev.,* 2013, **42**, 2824-2860. http://dx.doi.org/10.1039/c2cs35335k

43. S. Peng and K. Cho, *Nano Lett.,* 2003, **3**, 513-517. http://dx.doi.org/10.1021/nl034064u

44. S. Brahim, S. Colbern, R. Gump, A. Moser and L. Grigorian, *Nanotechnol.,* 2009, **20**, 1-7. http://dx.doi.org/10.1088/0957-4484/20/23/235502

45. Q. Zhao, M.B. Nardelli, W. Lu and J. Bernholc, *Nano Lett.,* 2005, **5**, 847-851. http://dx.doi.org/10.1021/nl050167w

46. A. Abdelhalim, A. Abdellah, G. Scarpa and P. Lugli, *Nanotechnol.,* 2014, **25**, 1-10. http://dx.doi.org/10.1088/0957-4484/25/5/055208

47. Z. Zanolli, R. Leghrib, A. Felten, J.J. Pireaux, E. Llobet and J.C. Charlier, *ACS Nano,* 2011, **5**, 4592-4599.
http://dx.doi.org/10.1021/nn200294h

48. I.V. Anoshkin, A.G. Nasibulin, P.R. Mudimela, M. He, V. Ermolov and E.I. Kauppinen, *Nano Res.,* 2013, **6**, 77-86.
http://dx.doi.org/10.1007/s12274-012-0282-6

49. M. Ding, Y. Tang, P. Gou, M.J. Reber and A. Star, *Adv. Mater.,* 2011, **23**, 536-540.
http://dx.doi.org/10.1002/adma.201003304

50. D.R. Kauffman, D.C. Sorescu, D.P. Schofield, B.L. Allen and K.D. Jordan, A. Star, *Nano Lett.,* 2010, **10**, 958-963.
http://dx.doi.org/10.1021/nl903888c

51. X. Mao, G.C. Rutledge and T.A. Hatton, *Nanotoday,* 2014, **9**, 405-432.
http://dx.doi.org/ 10.1016/j.nantod.2014.06.011

52. P. Gajendran and R. Saraswathi, *Pure Appl. Chem.,* 2008, **80**, 2377-2395.
http://dx.doi.org/10.1351/pac200880112377

53. V.K. Rana, S. Akhtar, S. Chatterjee, S. Mishra, R.P. Singh and C. S. Ha, *J. Nanosci. Nanotechnol.,* 2014, **14**, 2425-2435.
http://dx.doi.org/10.1166/jnn.2014.8498

54. V.K. Rana, M.C. Choi, J.Y. Kong, G.Y. Kim, M.J. Kim, S.H. Kim, S. Mishra, R.P. Singh, and C.S. Ha, *Macromol. Mater. Eng.,* 2011, **296**, 131-140.
http://dx.doi.org/10.1002/mame.201000307

55. A. Firouzi, S. Sobri, F.M. Yasin and F.L. Ahmadun, *Proceeding of the International Conference on Nanotechnology and Biosensors,* Singapore, 2011.
http://www.ipcbee.com/vol2/39-Y40002.pdf

56. H. Ago, N. Uehara, N. Yoshihara, M. Tsuji, M. Yumura, N. Tomonaga and T. Setoguchi, *Carbon,* 2006, **44**, 2912-2918. http://dx.doi.org/10.1016/j.carbon.2006.05.049

57. T. Yamada, T. Namai, K. Hata, D.N. Futaba, K. Mizuno, J. Fan, M. Yudasaka, M. Yumura and S. Iijima, *Nat. Nanotechnol.,* 2006, **1**, 131-136. http://dx.doi.org/doi:10.1038/nnano.2006.95

58. B. Yeole, T. Sen, D.P. Hansora and S. Mishra. *J. Appl. Polym. Sci.,* 2015*,* **132**, 1-9. http://dx.doi.org/10.1002/app.42379

59. J. Huang and R.B. Kaner, *Chem. Commun.,* 2006, **4**, 367-376. http://dx.doi.org/10.1039/b510956f

60. Z. Zanolli and J.C. Charlier, *ACS Nano* 2012, 6, 10786-10791. http://dx.doi.org/10.1021/nn304111a

61. Y. Shang, X. He, Y. Li, L. Zhang, Z. Li, C. Ji, E. Shi, P. Li, K. Zhu, Q. Peng, C. Wang, X. Zhang, R. Wang, J. Wei, K. Wang, H. Zhu, D. Wu and A. Cao, *Adv. Mater.,* 2012, **24**, 2896-2900. http://dx.doi.org/10.1002/adma.201200576

62. S. Mao, G. Lu and J. Chen, *J. Mater. Chem. A,* 2014, **2**, 5573-5579. http://dx.doi.org/10.1039/c3ta13823b

63. L. Hu, M. Pasta, F.L. Mantia, L. Cui, S. Jeong, H. Dawn, D. Jang, W. Choi, S.M. Han and Y. Cui, *Nano Lett.,* 2010, **10**, 708-714. http://dx.doi.org/10.1021/nl903949m

64. N. Liu, W. Ma, J. Tao, X. Zhang, J. Su, L. Li, C. Yang, Y. Gao, D. Golberg and Y. Bando*, Adv. Mater.,* 2013, **25**, 4925-4931. http://dx.doi.org/10.1002/adma.201301311

65. L. Kou, T. Huang, B. Zheng, Y. Han, X. Zhao, K. Gopalsamy, H. Sun and C. Gao, *Nat. Commun.,* 2014, **5**, 1-10. http://dx.doi.org/10.1038/ncomms4754

66. J. Zhong, Y. Zhang, Q. Zhong, Q. Hu, B. Hu, Z.L. Wang and J. Zhou, *ACS Nano,* 2014, **8**, 6273-6280. http://dx.doi.org/10.1021/nn501732z

67. S. Yao and Y. Zhu, *Nanoscale,* 2014, **6**, 2345-2352. http://dx.doi.org/10.1039/C3NR05496A

68. S. Jung, J. Lee, T. Hyeon, M. Lee and D.H. Kim, *Adv. Mater.,* 2014, **26**, 6329-6334. http://dx.doi.org/10.1002/adma.201402439

69. T. Yamada, Y. Hayamizu, Y. Yamamoto, Y. Yomogida, A.I. Najafabadi, D.N. Futaba and K. Hata, *Nat. Nanotechnol.,* 2011, **6**, 296-301. http://dx.doi.org/10.1038/nnano.2011.36

70. Y. Li, Y. Shang, X. He, Q. Peng, S. Du, E. Shi, S. Wu, Z. Li, P. Li and A. Cao, *ACS Nano,* 2013, **7**, 8128-8135. http://dx.doi.org/10.1021/nn403400c

71. W. Zeng, L. Shu, Q. Li, S. Chen, F. Wang and X.M. Tao, *Adv. Mater.,* 2014, **26**, 5310-5336. http://dx.doi.org/10.1002/adma.201400633

72. Y.H. Lee, J.S. Kim, J. Noh, I. Lee, H.J. Kim, S. Choi, J. Seo, S. Jeon, T.S. Kim, J.Y. Lee and J.W. Choi, *Nano Lett.,* 2013, **13**, 5753-5761. http://dx.doi.org/10.1021/nl403860k

73. P. Saini, V. Choudhary, *J. Appl. Polym. Sci.,* 2013, **129**, 2832-2839. http://dx.doi.org/10.1002/APP.38994

74. M. Melzer, J.I. Mönch, D. Makarov, Y. Zabila, G. Santiago C. Bermúdez, D. Karnaushenko, S. Baunack, F. Bahr, C. Yan, M. Kaltenbrunner and O.G. Schmidt, *Adv. Mater.,* 2014, **27**, 1274-1280.
http://dx.doi.org/10.1002/adma.201405027

Captions to Figures

Figure 1 Illustration of multi-step strategy for purification of CNTs

Figure 2 Steps for preparation of (a) γ-Fe_2O_3 nanoparticles and (b) PANi/γ-Fe_2O_3 composite films

Figure 3 Schematic representation of a two-probe gas sensing setup

Figure 4 FE-SEM micrographs [K1 (1 wt%), K2 (1.25 wt%), K3 (1.5 wt%)] and XRD pattern of catalyst (Fe/MgO) nanoparticles

Figure 5 FE-SEM micrographs of CNTs showing growth at 1000 ^oC and XRD pattern of CNTs showing crystalline behavior

Figure 6 Nano-fibrous morphology of PAni/γ-Fe_2O_3 composite films

Figure 7 Schematic view [Reprinted with permission from [63]. Copyright (2010) American Chemical Society], graphical view, photographic view and FE-SEM view of conductive cotton thread functionalized using CNTs

Figure 8 FE-SEM micrographs of multi-grade nanostructured thread [(a-b) 1 wt%, (c-d) 2 wt% and (e-f) 3 wt% loading of PAni/γ-Fe_2O_3 nanostructures]

Figure 9 FE-SEM micrograph of conductive thread embedded with 3 wt% PAni/γ-Fe_2O_3 nanostructures [(a) 3 wt%, (b) 5 wt% and (c) 10 wt% loading of CNT]

Figure 10 Current–voltage (I–V) characteristics of multi-grade nanostructured thread (a) virgin samples, (b) variation in CNT loading (c) variation in PAni/γ-Fe_2O_3 nanostructure loading

Figure 11 Current–time characteristics of (a) virgin samples, multi-grade nanostructured thread, (b) loaded with various wt% of CNT at constant wt% of PAni/γ-Fe_2O_3 nanostructures, (c) loaded with various wt% of PAni/γ-Fe_2O_3 nanostructures at constant wt% of CNT, (d) Magnification of image (b) showing Response time of

multi-grade nanostructured threads loaded with various wt% of CNT, (e) Magnification of image (c) showing Response time of multi-grade nanostructured threads loaded with various wt% of PAni/γ-Fe_2O_3 nanostructures

Figure 12 LPG sensing response values of multi-grade hybrid nanostructured thread

Figure 13 LPG sensing phenomena

Captions to Tables

Table 1 Composition of reactants used for preparation of catalyst nanoparticle

Table 2 Composition of reactants used for preparation of hybrid (CNT/PAni/γ-Fe_2O_3) nanostructured threads

Table 3 Yield and crystallinity of CNTs

Table 4 Sensing performances showing comparison between present work and previous reported work of LPG detection at different conditions

List of Tables

Table 1

Sample code	Weight ratio (Fe:MgO)	Percent weight ratio (%)	Quantity of $Fe(NO_3)_3 \cdot 9H_2O$ (gm)	Quantity of MgO (gm)
K1	1:10	0.1	4.04	4.04
K2	1.25:10	0.125	5.05	
K3	1.5:10	0.15	6.061	

Table 2

Sr. No.	Sample code	Quantity/Scale of material		
		CNT (mg)	PAni/γ-Fe_2O_3 nanostructures (mg)	Thread (cm)
1	CNT pellet	100	-	-
2	PANi/γ-Fe_2O_3 pellet	-	100	-
3	CNT/thread	50	-	5
4	PANi/γ-Fe_2O_3/thread	-	50	5
5	PANi/γ-Fe_2O_3/ CNT/cotton thread (Hybrid nanostructured thread)	25	75	5
6		50	75	5
7		75	75	5
8		100	75	5
9		100	100	5
10		100	125	5
11		100	150	5

Table 3

Sample code	Catalyst code	Weight of catalyst (gm)	Weight of product + catalyst (gm)	Weight of pure CNT purified (gm)	% of crystallinity (from XRD)
CNT1	K1	0.2	0.361	0.310	63.7
CNT2	K2		0.451	0.394	76.8
CNT3	K3		0.396	0.352	63.6

Table 4

Nanocomposite material	Concentration of LPG, ppm	Response value or % Response	Response time, sec	Recovery time, sec
Minimum concentration detection at room temperature				
CNT/PAni/γ-Fe_2O_3 nanostructured thread **present work**	50	0.91	~20-25	~35-40
PAni/γ-Fe_2O_3 [1]	50	0.5	60	~120
PAni/Y_2O_3 [6]	60-100	0.7-1.7	-	-
Nano-TiO_2 [13]	100	0.10	32	40
PAni-CMC [15]	50-100	~ 2-8 %	150	200
Maximum sensing factor or % response at room temperature				
PAni/n-CdS [3]	260	~5 %	210	90
PAni/n-TiO_2 [4]	400	15 %	200	135
PAni/ZnO [7]	1250	10 %	-	-

Polythiophene/SnO_2 [9]	5000	9.5 %	196	182
PAni/$ZnMoO_4$ [10]	800	20.6 %	400	24000
PAni/n-CdSe [12]	400	40 %	50	200
PAni/ZnO [14]	1000	~ 3	100	185
CdS/polyacrylamide [16]	10000	~180 %	1000	500
$Cd(NO_3)_2 \cdot (AAM)_4 \cdot 2H_2O$ [16]	10000	14000	120	480
$ZnFe_2O_4$ nanorods [17]	2000	140 %	60	300
CdS nanowires with PbS nanoparticles [18]	1200	60%	120	105
Maximum sensing factor or % response at higher temperature				
Fe_2O_3 modified SnO_2 nanostructures [2]	1000	1990 @ 350 ^oC	-	-
Nano-TiO_2 [5]	1250	~11 % @ 400 ^oC	-	-
Nano-ZnO [8]	500	~0.7 @ 200 ^oC	-	-
Nano-ZnO [11]	200	0.9 @ 100 ^oC	5	6